ELSEVIER

Thermochimica Acta 370 (2001) 37–48

thermochimica acta

www.elsevier.com/locate/tca

Application of the Avrami, Tobin, Malkin, and Urbanovici–Segal macrokinetic models to isothermal crystallization of syndiotactic polypropylene☆

Pitt Supaphol*

The Petroleum and Petrochemical College, Chulalongkorn University, Soi Chulalongkorn 12, Phyathai Road, Pathumwan, Bangkok 10330, Thailand

Received 26 June 2000; accepted 4 December 2000

Abstract

Various kinetic equations, namely the Avrami, Tobin, Malkin, and Urbanovici–Segal models, have been applied to describe the kinetics of primary crystallization from the melt state of syndiotactic polypropylene (s-PP) under isothermal conditions. Analysis was carried out using a data-fitting procedure, in which the experimental data were fitted directly to each model using a non-linear multi-variable regression program. The results suggested that the experimental data of s-PP can be best described by the Urbanovici–Segal model, followed by the Avrami, Malkin, and Tobin models, respectively.

Keywords: Isothermal crystallization; Kinetic equations; Avrami; Tobin; Malkin; Urbanovici–Segal; Syndiotactic polypropylene

1. Introduction

The overall crystallization process in semi-crystalline polymers can be divided into two main processes: primary crystallization and secondary crystallization. The primary crystallization process is the macroscopic development of crystallinity as a result of two consecutive microscopic mechanisms: primary nucleation and subsequent crystal growth. The secondary crystallization process is mainly concerned with the crystallization of interfibrillar, crystallizable melt, which was rejected and trapped between the fibrillar structure formed during the growth of crystalline aggregates (e.g. axialites, spherulites, etc.) [1,2]. If crystallization occurs at high enough temperatures and/or long enough time intervals, other types of secondary crystallization (i.e. crystal perfection and crystal thickening) may become significant enough to increase the ultimate absolute crystallinity.

In order to describe the macroscopic evolution of crystallinity during primary crystallization under quiescent isothermal conditions, a number of macrokinetic models have been proposed over the past 60 years: they are, for example, the so-called *Avrami* [3–9], the Tobin [10–12], the Malkin [13], and the Urbanovici–Segal equation [14]. Among these, the Avrami equation is the most widely used due partly to its mathematical simplicity, firm theoretical basis [15], and fair description of the experimental crystallization data in real polymer systems [16–18].

☆ Parts of the work were presented at the 58th Annual Technical Conference (ANTEC) of the Society of Plastics Engineers (SPE) held in Orlando, FL, USA during 7–11 May, 2000.

* Tel.: +66-2-218-4134; fax: +66-2-215-4459.
E-mail address: ps@sunsv1.ppc.chula.ac.th (P. Supaphol).

0040-6031/01/$ – see front matter
PII: S0040-6031(00)00767-X

Unlike the Avrami equation, use of the Tobin, Malkin, and Urbanovici–Segal to analyze the isothermal crystallization data of semi-crystalline polymers is uncommon. Qualitative comparison between the Avrami and Tobin models was performed on the isothermal crystallization data of poly(ethylene terephthalate) (PET), poly(phenylene sulfide) (PPS) [19], medium density polyethylene (MDPE), and poly(oxymethylene) (POM) [20], and that between the Avrami and Malkin models was carried out on the isothermal crystallization data of polyethylene (PE), isotactic polypropylene (*i*-PP), PET, poly(propylene oxide) (PPO), and polyurethane (PU) [13]. In addition, qualitative comparison between the Avrami and Urbanovici–Segal models was performed on the isothermal crystallization data of poly(L-lactic acid) (PLLA) [21].

Recently, qualitative comparison among the Avrami, Tobin, and Malkin equations was performed on the isothermal crystallization data of syndiotactic polypropylene (s-PP) [17,18]. The results showed that the Avrami equation was found to give the best description to the experimental data of s-PP, while the Malkin and Tobin equations were the second best and the worst, respectively. Unfortunately, qualitative comparison of the Urbanovici–Segal with the other three in describing the isothermal crystallization data of s-PP was not carried out in the previous reports [17,18], because the author did not become familiar with the Urbanovici–Segal equation [14,21] until very recently. It is, therefore, the objective of this study to compare the quality of the Avrami, Tobin, Malkin and Urbanovici–Segal models in describing the isothermal crystallization data of s-PP.

Since Urbanovici et al. [21] showed that the Urbanovici–Segal equation gives a better description of the isothermal crystallization data of PLLA than does the Avrami, it is hypothesized that the Urbanovici–Segal should provide better description of the isothermal crystallization of s-PP than do the other three as well. In order to verify this hypothesis, all of the aforementioned kinetic equations are used to analyze the isothermal crystallization data of s-PP using the *data-fitting procedure* [17] such that the experimental data are fitted to each respective equation by way of a non-linear multi-variable regression program. The degree of the fit suggests the applicability of the model in describing the isothermal crystallization data of s-PP.

2. Theoretical background

Traditionally, studies related to the overall kinetics of isothermal crystallization of semicrystalline polymers in DSC have been based on the information obtained from the crystallization exotherms [22–24], with an assumption that the evolution of crystallinity is linearly proportional to the evolution of heat released during the course of crystallization. Based on this assumption, the relative crystallinity as a function of time $\theta(t)$ can then be obtained by intergrating the crystallization exotherms according to the equation

$$\theta(t) = \frac{\int_0^t (\mathrm{d}H_\mathrm{c}/\mathrm{d}t)\,\mathrm{d}t}{\Delta H_\mathrm{c}} \in [0,1], \tag{1}$$

where t is the elapsed time during the course of crystallization, $\mathrm{d}H_\mathrm{c}$ the enthalpy of crystallization released during an infinitesimal time interval $\mathrm{d}t$, and ΔH_c is the total enthalpy of crystallization for a specific crystallization temperature, which is defined as

$$\Delta H_\mathrm{c} = \int_0^\infty (\mathrm{d}H_\mathrm{c}/\mathrm{d}t)\,\mathrm{d}t. \tag{2}$$

Analysis of the time-dependent relative crystallinity function $\theta(t)$ is usually carried out in the context of the Avrami equation [3–9], which can be expressed as

$$\theta(t) = 1 - \exp[-(K_\mathrm{a}t)^{n_\mathrm{a}}] \in [0,1], \tag{3}$$

where K_a is the Avrami rate constant, and n_a the Avrami exponent. Usually, the Avrami rate constant K_a is written in the form of the composite Avrami rate constant k_a (i.e. $k_\mathrm{a} = K_\mathrm{a}^n$). It was shown that k_a (the dimension of which is given in $(\mathrm{time})^{-n}$) is not only a function of temperature, but also a function of the Avrami exponent n_a [25]. As a result, use of K_a should be more preferrable than use of k_a due to partly to the facts that it is independent of the Avrami exponent n_a and its dimension is given in $(\mathrm{time})^{-1}$. It should be noted that both k_a (and hence K_a) and n_a are constants specific to a given crystalline morphology and type of nucleation for a particular crystallization condition [15] and that, based on the original assumptions of the theory, the value of the Avrami exponent n_a should be an integer, ranging from 1 to 4.

Aiming at improving the Avrami equation in describing the experimental data at the later stages of crystallization, Tobin [10–12] proposed a different expression describing the kinetics of phase transformation with an emphasis on growth impringement. The original theory was written in the form of a nonlinear Volterra integral equation, of which zeroth-order solution is given by

$$\theta(t) = \frac{(K_t t)^{n_t}}{1 + (K_t t)^{n_t}} \in [0, 1], \quad (4)$$

where K_t is the Tobin rate constant, and n_t the Tobin exponent. Based on this proposition, the Tobin exponent n_t needs not be integral [11,12], and it is mainly governed by different types of nucleation and growth mechanisms. It should be noted that, according to the original publications [10–12], the Tobin rate constant is written in the form of the composite Tobin rate constant k_t (i.e. $k_t = K_t^n$), which is not only a function of temperature, but also a function of the Tobin exponent n_t (similar to the case of k_a mentioned previously) [25]. As a result, use of K_t should be more preferable than use of k_t due partly to the facts that it is independent of the Tobin exponent n_t and its dimension is given in $(\text{time})^{-1}$.

Derived based on a postulation that the overall crystallization rate equals the summation of the rate at which the degree of crystallinity varies with the emergence of the primary nuclei and the rate of variation in the degree of crystallinity varies with the crystal growth rate, Malkin et al. [13] arrived at a totally different kinetic equation

$$\theta(t) = 1 - \frac{C_0 + 1}{C_0 + \exp(C_1 t)} \in [0, 1], \quad (5)$$

where C_0 is the Malkin exponent which relates directly to the ratio of the crystal growth rate G to the primary nucleation rate I (i.e. $C_0 \propto G/I$), and C_1 is the Malkin crystallization rate constant which relates directly to overall crystallization rate (i.e. $C_1 = aG + bI$, where a and b are specific constants). It should be noted that the dimension of the Malkin rate constant is given in $(\text{time})^{-1}$.

Recently, Urbanovici and Segal [14] proposed a new kinetic equation, which is essentially a generalization of the Avrami model. In this model, the relationship between the time-dependent relative crystallinity function $\theta(t)$ and the crystallization time t is given by

$$\theta(t) = 1 - [1 + (r - 1)(K_{us} t)^{n_{us}}]^{1/(1-r)} \in [0, 1], \quad (6)$$

where K_{us} and n_{us} are the Urbanovici–Segal crystallization rate constant and the Urbanovici–Segal exponent, respectively, and r is a parameter which satisfies the condition $r > 0$. At the condition where $r \to 1$, the Urbanovici–Segal equation becomes identical to the Avrami [14]. This may simply mean that the parameter r is merely a factor determining the degree of deviation of the Urbanovici–Segal model from the Avrami model. It is also worth noting that the Urbanovici–Segal kinetics parameters (i.e. K_{us} and n_{us}) have a similar physical meaning to the Avrami kinetics parameters (i.e. K_a and n_a), and that the dimension of K_{us} is also given in $(\text{time})^{-1}$.

3. Experimental details

3.1. Materials

The s-PP resin (labeled in this manuscript as s-PP#4) used in this study was supplied in pellet form by Fina Oil and Chemical Company (La Porte, TX, USA). Molecular characterization data, kindly measured by Dr. R.A. Phillips and his coworkers at Montell USA, Inc. (Elkton, MD, USA), gave the following molecular weight information: $M_n = 81{,}300$ Da, $M_w = 171{,}000$ Da, $M_z = 294{,}000$ Da, and $M_w/M_n = 2.1$. The syndiotacticity measured for this resin by the ^{13}C NMR spectroscopy gave the racemic pentad content (%rrrr) to be 74.6%, the racemic triad content (%rr) was 84.4%, and the racemic dyad content (%r) 89.2%.

3.2. Sample preparation

A film of s-PP sample was prepared from sliced pellets melt-pressed at 190°C between a pair of polyimide films which in turn were sandwiched between a pair of stainless steel platens, in a Wabash compression molding machine under a pressure of 4.62×10^2 MN m^{-2}. After 10 min holding time, the film approximately 285 μm thick, was taken out and

immediately quenched in an ice-water bath, while it was still between the two steel platens. This treatment assumed that previous thermal and mechanical histories formed during the pelletization process were essentially erased, and provided a controlled starting condition for our experiments.

3.3. Technique

A differential scanning calorimeter (Perkin-Elmer, DSC-7) was used to follow the isothermal crystallization. The DSC-7 equipped with internal cooling unit reliably provided a cooling rate up to 200°C min^{-1}. Temperature calibration was performed using an indium standard ($T_m^0 = 156.6°C$ and $\Delta H_f^0 = 28.5$ J g^{-1}). The consistency of the temperature calibration was checked every other run to ensure reliability and accuracy of the acquired data. To make certain that thermal lag between the polymer sample and the DSC sensors was kept to a minimum, each sample holder was loaded with a single disc, weighing 5.1 ± 0.3 mg, which was cut from the standard as-prepared film. Each sample was used only once and all the runs were carried out under nitrogen purge.

3.4. Experimental and analytical procedures

The experiment started by heating the sample from −40°C at a scanning rate of 80°C min^{-1} to 190°C where it was held for 5 min to ensure complete melting [26] before quenching at a cooling rate of 200°C min^{-1} to a specified isothermal crystallization temperature T_c. The crystallization exotherms were recorded for further analysis. The crystallization temperature T_c was varied from 70 to 95°C. The analysis of the experimental data was carried out using a nonlinear multi-variable regression program to directly fit the experimental data to the respective macrokinetic models (i.e. the data-fitting procedure [17]). The goodness of the fit is described by the chi-square parameter χ^2 [27], in which the lower the value is, the better will be the quality of the fit. According to this analytical procedure, corresponding parameters specified in each model are considered fitting parameters in the program and are provided by the program along with the best fits obtained.

4. Results and discussion

4.1. Isothermal crystallization of s-PP from the melt

Fig. 1 illustrates the time-dependent relative crystallinity function $\theta(t)$ (after subtraction of the induction time t_0) for four different crystallization temperatures T_c ranging from 75 to 95°C. It should be noted that the raw data are shown in Fig. 1 as different geometrical points, and that only 20 data points for each crystallization temperature were shown in order to attain good clarity of the plots. Evidently, the time to reach the ultimate crystallinity (i.e. complete crystallization) increased with increasing crystallization temperature T_c. An important bulk or overall kinetic parameter which can be determined directly from the $\theta(t)$ data is the half-time of crystallization $t_{0.5}$, which is defined as the elapsed time measured from the onset of crystallization until the crystallization is half-completed. Table 1 summarizes the values of crystallization half-time $t_{0.5}$ taken from the experimental $\theta(t)$ data.

According to Table 1, it is apparent that the half-time of crystallization $t_{0.5}$ increases assumingly exponentially with increasing crystallization temperature T_c, at least within the temperature range studied

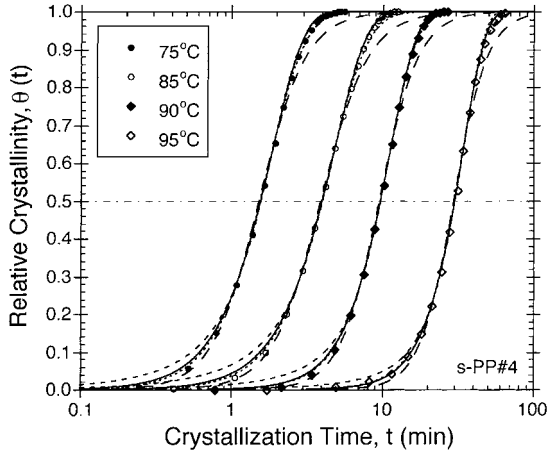

Fig. 1. Experimental relative crystallinity as a function of time of s-PP#4 for four crystallization temperatures. The experimental data, shown as various geometrical points, were fitted to the Avrami, Tobin, Malkin, and Urbanovici–Segal macrokinetic models, in which the best fits according to these models are shown as the solid, long-dashed, dashed, and dotted lines, respectively.

Table 1
Summary of the half-time of crystallization $t_{0.5}$, the reciprocal half-time $t_{0.5}^{-1}$, the Avrami kinetics parameters (i.e. n_a and K_a), and the χ^2 parameter suggesting the quality of the fit

T_c (°C)	$t_{0.5}$ (min)	$t_{0.5}^{-1}$ (min^{-1})	K_a^* (min^{-1})	n_a	K_a (min^{-1})	χ^2
70.0	1.2	8.10×10^{-1}	6.81×10^{-1}	2.12	6.81×10^{-1}	3.15×10^{-4}
72.5	1.3	7.53×10^{-1}	6.28×10^{-1}	2.02	6.28×10^{-1}	1.32×10^{-3}
75.0	1.6	6.42×10^{-1}	5.36×10^{-1}	2.05	5.32×10^{-1}	5.85×10^{-3}
77.5	1.9	5.40×10^{-1}	4.48×10^{-1}	1.98	4.46×10^{-1}	7.09×10^{-3}
80.0	2.6	3.89×10^{-1}	3.24×10^{-1}	1.98	3.21×10^{-1}	1.16×10^{-2}
82.5	3.1	3.20×10^{-1}	2.68×10^{-1}	2.07	2.64×10^{-1}	2.73×10^{-2}
85.0	4.0	2.49×10^{-1}	2.08×10^{-1}	2.01	2.07×10^{-1}	8.20×10^{-3}
87.5	6.8	1.47×10^{-1}	1.22×10^{-1}	2.03	1.22×10^{-1}	3.94×10^{-3}
90.0	9.8	1.02×10^{-1}	8.80×10^{-2}	2.48	8.80×10^{-2}	2.29×10^{-3}
92.5	16.3	6.14×10^{-2}	5.31×10^{-2}	2.54	5.30×10^{-2}	1.17×10^{-3}
95.0	30.4	3.29×10^{-2}	2.90×10^{-2}	2.91	2.91×10^{-2}	3.46×10^{-3}

(see Fig. 2). Also shown in Fig. 2 is a plot of the inverse value of the crystallization half-time (i.e. the reciprocal half-time $t_{0.5}^{-1}$) versus T_c, which is regarded as the most fundamental representation of the bulk crystallization rate of a semi-crystalline polymer. In cases where $t_{0.5}$ data can be measured accurately over the whole temperature range in which polymers can crystallize (i.e. $T_g < T_c < T_m^0$), the plot of $t_{0.5}$ versus T_c is expected to exhibit the typical bell-shaped curve, which is characterized by the nucleation control effect at low degrees of undercooling (i.e. $\Delta T = T_m^0 - T_c$) and the diffusion control effect at high degrees of undercooling.

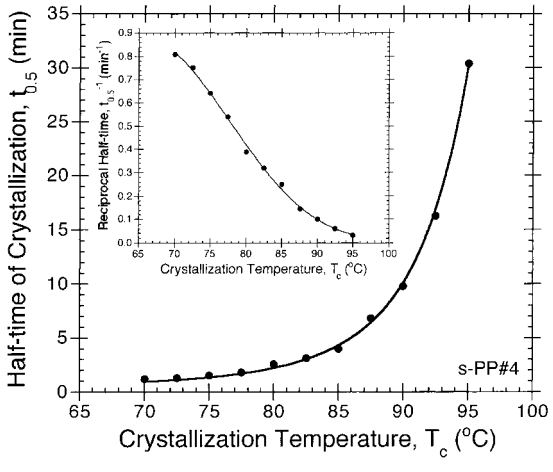

Fig. 2. Half-time of crystallization as a function of crystallization temperature, with the inset figure illustrating the reciprocal half-time as a function of crystallization temperature.

In a recent study on another s-PP resin (labelled therein as s-PP#1) [25], it was shown that an unmistakable, double bell-shaped curve was observed for the case of crystallization from the melt state (i.e. melt-crystallization) when the overall crystallization rate parameters were plotted as a function of the crystallization temperature. On the contrary, for the case of crystallization from the glassy state (i.e. cold-crystallization), only the typical bell-shaped curve was discernible. In order to account for the two maxima observed in the overall crystallization rate curve (i.e. at $T_c \approx 30$ and 60°C) for the case of crystallization from the melt, it was hypothesized that the high-temperature maximum (i.e. at $T_c \approx 60$°C) should relate to the maximum in the linear growth rate data, while the low-temperature maximum (i.e. at $T_c \approx 30$°C) to the maximum in the primary nucleation rate data. The fact that the plot of the linear growth rate data versus T_c exhibits only one maximum at $T_c \approx 70$°C [28] provides a proof that the above hypotheses sound reasonable.

Since, for the case of s-PP#4, it is not possible to collect accurately the data over the whole temperature range due to premature crystallization occurring when $T_c < 70$°C, whether or not the double bell-shaped curve should be experimentally observed, when crystallizing from the melt state, is immaterial. It can only be established at this point that, within the temperature range studied (i.e. 70°C $\leq T_c \leq$ 95°C),

s-PP#4 crystallizes in the region where nucleation mechanism is the rate determining step.

4.2. Isothermal crystallization kinetics based on the Avrami analysis

Data analysis based on the Avrami kinetic equation is carried out by directly fitting the experimental $\theta(t)$ data obtained for each crystallization temperature to Eq. (3) (shown in Fig. 1 as dashed lines). As a result, the Avrami kinetics parameters (i.e. n_a and K_a) along with the χ^2 parameter were obtained. These parameters are summarized in Table 1. The Avrami exponent n_a calculated for $\theta(t) \in [0.1, 0.8]$ is found to range from ca. 2.0 to 2.9, which, according to the definition of the Avrami exponent [15], may correspond to a two dimensional growth with a combination of the thermal and athermal nucleation mechanisms (to pacify the fractional values of the Avrami exponent observed). Intuitively, the temperature-dependence of the Avrami exponent n_a, within the nucleation control region, should be such that n_a increases with increasing T_c. This is because the number of the athermal nuclei is found to increase tremendously with decreasing crystallization temperature T_c [26,29], causing the nucleation mechanism to be more instantaneous in time which decreases the values of the Avrami exponent n_a.

According to Table 1, the Avrami rate constant K_a is found to decrease monotonically with increasing crystallization temperature T_c, suggesting that s-PP crystallizes faster with decreasing T_c. This remark is only valid when the T_c of interest is in the range where nucleation mechanism is the rate determining step (i.e. $T_c \geq$ ca. 60°C for s-PP). A similar implication was addressed earlier based on the fact that the reciprocal half-time $t_{0.5}^{-1}$ also shows the same trend (see inset figure in Fig. 2). In fact, the Avrami rate constant K_a can be calculated directly from the reciprocal half-time $t_{0.5}^{-1}$ according to the following equation:

$$K_a = (\ln 2)^{1/n_a} t_{0.5}^{-1}. \tag{7}$$

The calculated values of the Avrami rate constant (k_a^*) are also summarized in Table 1 for comparison. Evidently, good agreement between the experimental rate constant K_a and the calculated rate constant K_a^* is observed, with the calculated values being ca. 0.4% greater than the experimental values on average.

Recently, Ding and Spruiell [9] derived an equation describing the evolution of crystallinity of semi-crystalline polymers based on the traditional notion of primary nucleation and subsequent crystal growth mechanisms and arrived at a similar expression to that of the Avrami model. The uniqueness of the Ding–Spruiell version of the Avrami model is represented by (1) the introduction of the *nucleation rate function* $I(t)$ (to quantify the nucleation rate I as a function of time throughout the course of crystallization):

$$I(t) = I_c(1 + m)t^m, \tag{8}$$

where I_c is the *nucleation rate constant* (a temperature-dependent, but time-independent, parameter, the dimension of which is given in (number of nuclei/(s^{m+1} cm^3)), and m is the *nucleation index*; and (2) the new and more thorough mathematical definitions of the Avrami kinetics parameters:

$$n_a = n + m + 1, \tag{9}$$

and

$$k_a = nC_nI_cG^nB(m + 2, n), \tag{10}$$

where n is the geometric or dimensionality index (e.g. $n = 1$ for rod, $n = 2$ for disc, and $n = 3$ for sphere), C_n is the shape factor (e.g. $C_2 = \pi$ and $C_3 = 4\pi/3$, G is the crystal growth rate, and $B(m + 2, n)$ denotes the B-function well-defined in the original publication [9]. It should be addressed at this point again that the composite Avrami rate constant k_a shown in Eq. (10) relates to the Avrami rate constant K_a shown in Eq. (3) according to the relationship: $k_a = K_a^n$, as previously mentioned.

According to Eq. (9), the traditional sense of the Avrami exponent n_a in describing the dimensionality of the crystal geometry is restored with the geometric or dimensionality index n, but, more importantly, abnormality in the experimental observation of the Avrami exponent n_a (viz. fractional values of n_a, or values of n_a greater than 4) can now be theoretically explainable by the introduction of the nucleation index m. Although the nature of the nucleation index m is not entirely understood at the present time and is a subject of further investigation, the qualitative description of the nucleation index m (for a fixed value of the geometric index n) in describing the nucleation mechanism throughout the course of the crystallization process is summarized in Table 2.

Table 2
Qualitative description of the nucleation index m

	Nucleation mechanism	Nature of the nucleation rate over crystallization time
$m = -1$	Instantaneous	Constant
$-1 < m < 0$	Instantaneous and sporadic	Gradually decreasing with time and approaching a constant value at a certain time
$m = 0$	Sporadic	Steadily increasing with time
$0 < m < 1$	Sporadic	Increasing with time
$m > 1$	Sporadic	Increasing strongly with time

4.3. Isothermal crystallization kinetics based on the Tobin analysis

Data analysis based on the Tobin kinetic equation is carried out by directly fitting the experimental $\theta(t)$ data obtained for each crystallization temperature to Eq. (4) (shown in Fig. 1 as long-dashed lines). Table 3 summarizes the Tobin kinetics parameters (i.e. n_t and k_t) along with the χ^2 parameter obtained as a result of the best fit. According to Table 3, the Tobin exponent n_t, also calculated for $\theta(t) \in [0.1, 0.8]$, is found to range from ca. 2.7 to 3.9. By comparison, it is apparent that, at any crystallization temperature, the Tobin exponent n_t is consistently greater in value than the Avrami exponent n_a. On average, the difference between the Tobin exponent n_t and the Avrami exponent n_a is roughly 0.8 (i.e. $n_t - n_a \approx 0.8$), which is in general accordance with other observations reported elsewhere [17–20].

According to Table 3, the Tobin rate constant K_t apparently exhibits a similar trend to that suggested by the reciprocal half-time $t_{0.5}^{-1}$ and the Avrami rate constant K_a in that it decreases with increasing crystallization temperature. Like the Avrami rate constant K_a, the Tobin rate constant K_t can be calculated directly from the reciprocal half-time $t_{0.5}^{-1}$ according to the following equation

$$K_t = t_{0.5}^{-1}. \tag{11}$$

The calculated values of the Tobin rate constant (k_t^*) are also summarized in Table 3 for comparison. Evidently, good agreement is observed between the experimental rate constant K_t and the calculated rate constant K_t^*, with the calculated values being ca. 1.7% less than the experimental values on average.

4.4. Isothermal crystallization kinetics based on the Malkin analysis

Data analysis based on the Malkin kinetic equation is carried out by directly fitting the experimental $\theta(t)$ data obtained for each crystallization temperature to Eq. (5) (shown in Fig. 1 as dashed lines). Table 4 summarizes the Malkin kinetics parameters (i.e. C_0 and C_1) along with the χ^2 parameter obtained as a result of the best fit. According to Table 4, the Malkin

Table 3
Summary of the reciprocal half-time $t_{0.5}^{-1}$, the Tobin kinetics parameters (i.e. n_t and K_t), and the χ^2 parameter suggesting the quality of the fit

T_c (°C)	$t_{0.5}^{-1}$ (min^{-1})	K_t^* (min^{-1})	n_t	K_t (min^{-1})	χ^2
70.0	8.10×10^{-1}	8.10×10^{-1}	2.88	8.27×10^{-1}	3.67×10^{-2}
72.5	7.53×10^{-1}	7.53×10^{-1}	2.75	7.70×10^{-1}	3.44×10^{-2}
75.0	6.42×10^{-1}	6.42×10^{-1}	2.80	6.51×10^{-1}	2.73×10^{-2}
77.5	5.40×10^{-1}	5.40×10^{-1}	2.71	5.50×10^{-1}	3.39×10^{-2}
80.0	3.89×10^{-1}	3.89×10^{-1}	2.70	3.96×10^{-1}	4.46×10^{-2}
82.5	3.20×10^{-1}	3.20×10^{-1}	2.85	3.22×10^{-1}	3.35×10^{-2}
85.0	2.49×10^{-1}	2.49×10^{-1}	2.75	2.54×10^{-1}	3.62×10^{-2}
87.5	1.47×10^{-1}	1.47×10^{-1}	2.76	1.49×10^{-1}	6.95×10^{-2}
90.0	1.02×10^{-1}	1.02×10^{-1}	3.36	1.04×10^{-1}	5.24×10^{-2}
92.5	6.14×10^{-2}	6.14×10^{-2}	3.43	6.23×10^{-2}	8.24×10^{-2}
95.0	3.29×10^{-2}	3.29×10^{-2}	3.89	3.35×10^{-2}	1.73×10^{-2}

Table 4
Summary of the Malkin kinetics parameters (i.e. C_0 and C_1) and the χ^2 parameter suggesting the quality of the fit

T_c (°C)	C_0	C_1 (min^{-1})	χ^2	C_0^*	C_1^* (min^{-1})
70.0	15.89	2.32	1.10×10^{-2}	14.98	2.29
72.5	12.98	2.02	1.68×10^{-2}	12.46	2.01
75.0	13.60	1.74	2.97×10^{-2}	13.09	1.74
77.5	11.84	1.40	3.75×10^{-2}	11.50	1.40
80.0	11.77	1.01	5.53×10^{-2}	11.46	1.01
82.5	14.17	0.87	8.60×10^{-2}	13.68	0.88
85.0	12.58	0.66	4.06×10^{-2}	12.18	0.66
87.5	13.19	0.39	3.61×10^{-2}	12.67	0.39
90.0	29.79	0.35	1.92×10^{-2}	27.28	0.34
92.5	33.01	0.22	1.83×10^{-2}	30.04	0.21
95.0	59.25	0.14	3.87×10^{-3}	52.63	0.13

exponent C_0 is found to range from ca. 11.8 to 59.3. Fundamentally, the Malkin exponent C_0, which relates directly to the Avrami exponent n_a according to the following expression [13]

$$C_0 = 4^{n_a} - 4, \tag{12}$$

should exhibit a similar temperature-dependence to that of the Avrami exponent n_a. Such a remark is evident and can be deduced from the results summarized in Table 4. Additionally, the Malkin rate constant C_1 (see Table 4) exhibits a similar dependence on the crystallization temperature to the other bulk crystallization rate constants determined earlier. This is not surprising since the Malkin rate constant C_1 relates to the Avrami kinetics parameters (i.e. n_a and K_a) according to the following expression [13]

$$C_1 = \frac{\ln(4^{n_a} - 2)}{(\ln 2)^{1/n_a}} K_a. \tag{13}$$

Unlike the Avrami and Tobin kinetic equations, there is no direct analytical procedure for determining the Malkin kinetics parameters. Without the use of the data-fitting procedure to determine the Malkin kinetics parameters (i.e. C_0 and C_1), they can only be estimated from Eqs. (12) and (13), if the Avrami kinetics parameters are a priori known. The estimated values of the Malkin kinetics parameters (i.e. C_0^* and C_1^*) are also summarized in Table 4 for comparison. On average, the estimated values of the Malkin exponent (C_0^*) are found to be ca. 5.3% less than the experimental ones C_0, while the estimated values of the Malkin rate constant (C_1^*) are found to be ca. 0.6% less than the experimental ones C_1. Like the other two rate constants, the Malkin rate constant C_1 can also be calculated directly from the reciprocal half-time $t_{0.5}^{-1}$, along with a priori knowledge of the Avrami exponent n_a, according to the following equation

$$C_1 = \ln(4^{n_a} - 2) t_{0.5}^{-1}. \tag{14}$$

Though not listed in Table 4, the calculated values C_1^{**} are found to be exactly identical to the estimated values C_1^*. It is worth noting that, according to Eq. (14), the Malkin rate constant C_1 is not only a function of the reciprocal half-time $t_{0.5}^{-1}$, but also a function of the Avrami exponent n_a.

4.5. Isothermal crystallization kinetics based on the Urbanovici–Segal analysis

Analogous to the previous three cases, data analysis based on the Urbanovici–Segal kinetic equation is carried out by directly fitting the experimental $\theta(t)$ data obtained for each crystallization temperature to Eq. (6) (shown in Fig. 1 as dotted lines). Table 5 summarizes the Urbanovici–Segal kinetics parameters (i.e. n_{us}, K_{us}, and r) along with the χ^2 parameter obtained as a result of the best fit. According to Table 5, the Urbanovici–Segal exponent n_{us}, also calculated for $\theta(t) \in [0.1, 0.8]$, is found to range from ca. 2.1 to 2.8. The Urbanovici–Segal rate constant K_{us} apparently exhibits a similar trend to that suggested by the other crytallization rate parameters in that it decreases with increasing crystallization temperature. Like the Avrami rate constant K_a, the Urbanovici–Segal rate constant K_{us} can be calculated directly from

Table 5
Summary of the reciprocal half-time $t_{0.5}^{-1}$, the Urbanovici–Segal kinetics parameters (i.e. n_{us}, K_{us}, and r), and the χ^2 parameter suggesting the quality of the fit

T_c (°C)	$t_{0.5}^{-1}$ (min^{-1})	K_{us}^* (min^{-1})	n_{us}	K_{us} (min^{-1})	r	χ^2
70.0	8.10×10^{-1}	6.91×10^{-1}	2.17	6.92×10^{-1}	1.06	7.42×10^{-5}
72.5	7.53×10^{-1}	6.46×10^{-1}	2.11	6.48×10^{-1}	1.13	3.20×10^{-4}
75.0	6.42×10^{-1}	5.68×10^{-1}	2.24	5.68×10^{-1}	1.27	7.65×10^{-4}
77.5	5.40×10^{-1}	4.76×10^{-1}	2.16	4.77×10^{-1}	1.27	1.12×10^{-3}
80.0	3.89×10^{-1}	3.45×10^{-1}	2.17	3.44×10^{-1}	1.28	2.47×10^{-3}
82.5	3.20×10^{-1}	2.92×10^{-1}	2.40	2.91×10^{-1}	1.43	3.41×10^{-3}
85.0	2.49×10^{-1}	2.20×10^{-1}	2.20	2.21×10^{-1}	1.27	1.99×10^{-3}
87.5	1.47×10^{-1}	1.26×10^{-1}	2.12	1.26×10^{-1}	1.13	1.98×10^{-3}
90.0	1.02×10^{-1}	9.00×10^{-2}	2.59	9.03×10^{-2}	1.12	8.37×10^{-4}
92.5	6.14×10^{-2}	5.36×10^{-2}	2.58	5.34×10^{-2}	1.04	9.32×10^{-4}
95.0	3.29×10^{-2}	2.84×10^{-2}	2.80	2.85×10^{-2}	0.88	5.99×10^{-4}

the reciprocal half-time $t_{0.5}^{-1}$ according to the following equation

$$K_{us} = \left(\frac{0.5^{(1-r)} - 1}{r - 1}\right)^{1/n_{us}} t_{0.5}^{-1}. \quad (15)$$

The calculated values of the Urbanovici–Segal rate constant (K_{us}^*) are also summarized in Table 5 for comparison. Evidently, extremely good agreement is observed between the experimental rate constant K_{us} and the calculated rate constant K_{us}^*, with the calculated values being ca. 0.04% less than the experimental values on average.

Comparison between the kinetics parameters obtained from the Avrami and Urbanovici–Segal models (see Tables 1 and 5, respectively) indicates that the extent of the discrepancy between the Urbanovici–Segal and Avrami kinetics parameters depends significantly on the value of the parameter r obtained. It was stated elsewhere in this manuscript that the Urbanovici–Segal model becomes identical to the Avrami model when r approaches 1 [14]. According to Tables 1 and 5, when $r > 1$, the values of the Urbanovici–Segal kinetics parameters are systematically greater than those of the Avrami ones, as the greater the value of r is from 1, the larger the discrepancy between the values of the Urbanovici–Segal and the Avrami kinetics parameters becomes. It is apparent, according to Tables 1 and 5 that, when $r = 1.04$ (at $T_c = 92.5$°C), the difference between n_{us} and n_a is only 1.5% (see Fig. 3) and that between K_{us} and K_a is only 0.9%; whereas, when $r = 1.43$ (at $T_c = 82.5$°C), the qualitative difference between n_{us} and n_a is as much as 15.7% (see Fig. 3) and that between K_{us} and K_a is as much as 10.4%. On the contrary, when $r < 1$, the values of the Urbanovici–Segal kinetics parameters are systematically less than those of the Avrami ones. It is obvious, according to Tables 1 and 5 that, when $r = 0.88$ (at $T_c = 95$°C), the difference between n_{us} and n_a is −3.9% (see Fig. 3) and that between K_{us} and K_a is −2.2%.

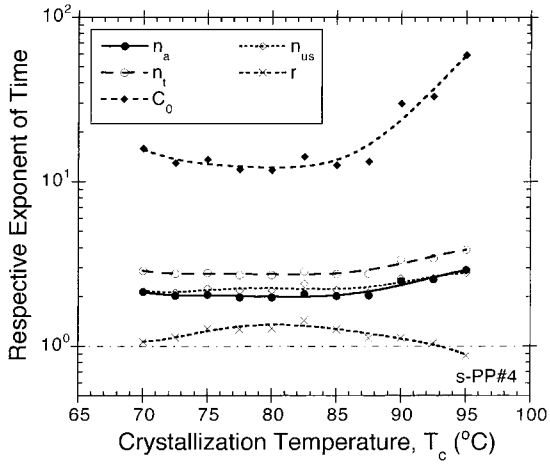

Fig. 3. The Avrami, Tobin, Malkin, and Urbanovici–Segal exponents of time and the parameter r as a function of crystallization temperature.

4.6. Qualitative comparison among the four Macrokinetic equations

The quality of each kinetic equation in describing the experimental $\theta(t)$ data is quantitatively represented by the value of the χ^2 parameter obtained along with the best fit, in which the lower the value is, the better will be the quality of the fit. Comparison of the values of the χ^2 parameter summarized in Tables 1, 3, 4 and 5 indicates that the Urbanovici–Segal model gave the best description of the experimental data, followed by the Avrami, Malkin, and Tobin models, respectively. Graphically, deviation of the fits according to the Malkin and Tobin models (shown in Fig. 1 as dashed and long-dashed lines, respectively) from the experimental data (shown in Fig. 1 as different geometrical points) is obvious, while that according to the Avrami and Urbanovici–Segal models (shown in Fig. 1 as solid and dotted lines) from the experimental data is much less pronounced.

Specifically, the Malkin model appears to over-estimate the $\theta(t)$ data at the early stage of crystallization (i.e. $\theta(t) \leq$ ca. 0.2), while the Tobin model appears to under-estimate the $\theta(t)$ data at the later stage of crystallization (i.e. $\theta(t) \geq$ ca. 0.8). If one is to compare the quality of the fits as described by the Avrami and Urbanovici–Segal models, one may from Fig. 1 that the Avrami model appears to over-estimate the $\theta(t)$ data at the early and the later stages of crystallization, respectively (i.e. $\theta(t) \leq$ ca. 0.2 and $\theta(t) \geq$ ca. 0.8, respectively).

4.7. Further discussion on temperature-dependence of the kinetics parameters

Fig. 3 illustrates the variation of all the kinetics exponents of time (i.e. n_a, n_t, C_0, and n_{us}) along with the parameter r as a function of the crystallization temperature. Apparently, each respective plot indicates that each respective exponent of time is roughly independent of temperature within the range $70^\circ\text{C} \leq T_c \leq$ ca. 87.5°C, while it increases with increasing crystallization temperature within the range ca. $87.5^\circ\text{C} \leq T_c \leq 95^\circ$C. The reason for this variation has been addressed elsewhere in this manuscript. Fig. 4 illustrates the temperature-dependence of all the bulk crystallization rate parameters (i.e. $t_{0.5}^{-1}$, K_a, K_t, C_1, and K_{us}). It is apparent that all of the bulk crystallization rate parameters exhibit a similar temperature-dependence. This similarity is understandable when one considers the facts that the units of these rate parameters are given in (min^{-1}) and that all of the crystallization rate parameters relate to the reciprocal half-time $t_{0.5}^{-1}$ according to Eqs. (7), (11), (14) and (15), respectively.

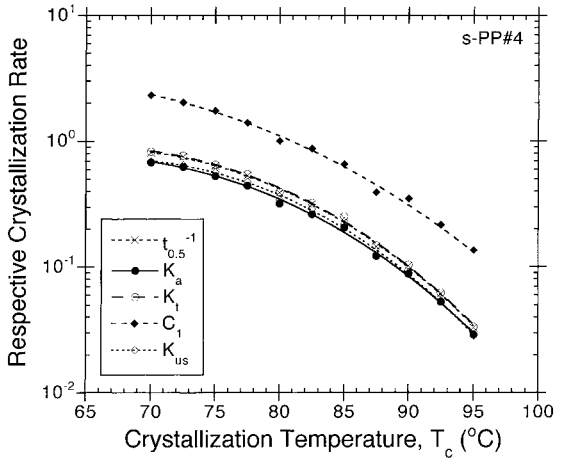

Fig. 4. Various crystallization rate parameters as a function of crystallization temperature. The experimental data, shown as various geometrical points, were fitted to Eq. (16), and the best fits are shown as various lines.

It is well accepted in the literature [17,25] that the bulk crystallization rate parameters (e.g. $t_{0.5}^{-1}$, K_a, K_t, C_1, and K_{us}) relate, in one way or another, to the primary nucleation rate I and/or the subsequent crystal growth rate G [30–33], the temperature-dependence of the bulk rate parameter can accordingly be quantified and described. Even though the temperature-dependence of the parameters I and G are known to have a different temperature-dependence [30–33], the bulk crystallization rate parameters have often been taken to have a similar temperature-dependence to that of the subsequent crystal growth rate G (written in the context of the original Lauritzen and Hoffman secondary nucleation theory (LH theory) [32,33]), which can be expressed as

$$\Psi(T) = \Psi_0 \exp\left\{-\frac{A}{R(T_c - (T_g - C))} - \frac{B}{T_c(\Delta T)f}\right\}, \tag{16}$$

Table 6
Fitting parameters for the best possible fits of the respective rate parameters according to Eq. (16)

C (K)	Ψ_0	A (cal mol^{-1})	B (K^2)	χ^2
$t_{0.5}^{-1}$ (min^{-1})				
30	2.40×10^{18}	2890.4	8.53×10^5	1.82×10^{-3}
50	1.49×10^{20}	4233.2	8.81×10^5	1.84×10^{-3}
K_a (min^{-1})				
30	1.52×10^{17}	2631.4	8.13×10^5	1.29×10^{-3}
50	6.45×10^{18}	3852.8	8.38×10^5	1.30×10^{-3}
K_t (min^{-1})				
30	1.62×10^{18}	2843.6	8.47×10^5	2.00×10^{-3}
50	9.38×10^{19}	4164.4	8.75×10^5	2.02×10^{-3}
C_1 (min^{-1})				
30	1.33×10^{12}	1377.0	6.08×10^5	1.75×10^{-2}
50	9.16×10^{12}	2011.8	6.21×10^5	1.76×10^{-2}
K_{us} (min^{-1})				
30	7.41×10^{19}	3275.5	9.05×10^5	1.58×10^{-3}
50	8.05×10^{21}	4798.1	9.37×10^5	1.60×10^{-3}

where $\Psi(T)$ and Ψ_0 are the respective crystallization rate parameters (i.e. $t_{0.5}^{-1}$, K_a, K_t, C_1, and K_{us}) and the respective pre-exponential parameter (i.e. $(t_{0.5}^{-1})_0$, $K_{a,0}$, $K_{t,0}$, $C_{1,0}$, or $K_{us,0}$), respectively. A is a parameter related to the activation energy characterizing the molecular diffusion across the melt/crystal interface, while B is a parameter related to the secondary nucleation. T_g is the glass transition temperature (for s-PP, $T_g \approx 6.1^\circ$C [34]), C is the parameter which determines the temperature where the cessation of long-range molecular motion is expected (i.e. $T_g - C$) and is often taken to be either ca. 30 K or ca. 50 K below the glass transition temperature, R is the universal gas constant, ΔT is the degree of undercooling (i.e. $\Delta T = T_m^0 - T_c$; where, for s-PP, $T_m^0 \approx 168.7^\circ$C [34]), and finally f is a factor used to correct for the temperature-dependence of the heat of fusion (i.e. $2T_c/(T_c + T_m^0)$).

With the aid of Eq. (16), the temperature-dependent crystallization rate function $\Psi(T)$ can be determined by fitting each respective crystallization rate parameter (i.e. $t_{0.5}^{-1}$, K_a, K_t, C_1, or K_{us}) collected at various crystallization temperatures to Eq. (16) using the same non-linear multi-variable regression program. In order to obtain the best possible fits for the rate parameters with Eq. (16), the value of the parameter C was chosen to be either 30 or 50 K, while those of T_g and T_m^0 are fixed as previously noted. In so doing, the only unknown parameters which are provided by the program along with the best fits are Ψ_0, A, and B. Plots of the crystallization rate parameters of interest (i.e. $t_{0.5}^{-1}$, K_a, K_t, C_1, and K_{us}) and their corresponding best fit are illustrated in Fig. 4, while the values of the fitting parameters (i.e. Ψ_0, A, and B) along with the χ^2 parameter are summarized in Table 6. Examination of the values of the χ^2 parameter listed in Table 6 suggests to us that the goodness of the fits of these rate parameters according to Eq. (16) is very satisfactory. Interestingly, the values of all of the fitting parameters obtained when using $C = 50$ K were greater than those obtained when using $C = 30$ K. According to the values of the χ^2 parameter listed in Table 6, it can also be concluded that the quality of the fits, when using $C = 30$ K, were better than those, when using $C = 50$ K.

5. Conclusions

In this manuscript, a non-linear multi-variable regression program was used to fit the isothermal crystallization measurements obtained from the DSC to four kinetic equations; namely the Avrami, Tobin, Malkin, and Urbanovici–Segal; and was found to give reliable kinetics results. It was found that the quality of each, judging from the values of the

χ^2 parameter, in describing the isothermal crystallization data of s-PP falls in the following order: (1) the Urbanovici–Segal model, (2) the Avrami model, (3) the Malkin model, and (4) the Tobin model. This led to the rejection of the Tobin model in describing the isothermal crystallization data of s-PP.

The Avrami exponent was found to be in the approximate range of ca. 2.0 to 2.9, suggesting a *two dimensional growth* from a combination of thermal and athermal nuclei (i.e. instantaneous and sporadic nucleation mechanisms). All of the crystallization rate parameters (i.e. $t_{0.5}^{-1}$, K_a, K_t, C_1, and K_{us}) were found to be very sensitive to changes in the crystallization temperature. Within the crystallization temperature range studied (i.e. $70^\circ C \leq T_c \leq 95^\circ C$), the values of the rate parameters were all found to increase with decreasing temperature, due to the fact that s-PP crystallizes faster at lower temperature than at the higher temperature. Comparison with earlier results [17,18,34,35] suggested that the range of temperature in this study falls in the region where nucleation mechanism is the rate determining step.

It was also shown that all of the bulk crystallization rate parameters (i.e. $t_{0.5}^{-1}$, K_a, K_t, C_1, and K_{us}) have a finite, definable relationship with the crystallization temperature T_c (or the degree of undercooling ΔT), in which they can be described based on an equation similar to that proposed by Hoffman and coworker [32,33] for the temperature-dependence characteristic of the linear crystal growth rate of semi-crystalline polymers.

Acknowledgements

The author would like to thank Dr. J. Schardl of Fina Oil and Chemical Company (Dallas, TX, USA) for supplying the s-PP resin used in this study, and Dr. R.A. Phillips and his coworkers of Montell USA, Inc. (Elkton, MD, USA) for their kind assistance on molecular weight and tacticity characterization. In addition, a grant provided by chulalongtorn university through the development grants for new faculty/researchers is greatly acknowledged.

References

[1] H.D. Keith, F.J. Padden, J. Appl. Phys. 35 (1964) 1270.
[2] H.D. Keith, F.J. Padden, J. Appl. Phys. 35 (1964) 1286.
[3] A.N. Kolmogorov, Izvestiya Akad. Nauk USSR, Ser. Mater. 1 (1937) 355.
[4] W.A. Johnson, K.F. Mehl, Trans. Am. Inst. Mining Met. Eng. 135 (1939) 416.
[5] M.J. Avrami, Chem. Phys. 7 (1939) 1103.
[6] M.J. Avrami, Chem. Phys. 8 (1940) 212.
[7] M.J. Avrami, Chem. Phys. 9 (1941) 177.
[8] U.R. Evans, Trans. Faraday Soc. 41 (1945) 365.
[9] Z. Ding, J.E. Spruiell, J. Polym. Sci., Polym. Phys. 35 (1997) 1077.
[10] M.C. Tobin, J. Polym. Sci., Polym. Phys. 12 (1974) 399.
[11] M.C. Tobin, J. Polym. Sci., Polym. Phys. 14 (1976) 2253.
[12] M.C. Tobin, J. Polym. Sci., Polym. Phys. 15 (1977) 2269.
[13] A.Y. Malkin, V.P. Beghishev, I.A. Keapin, S.A. Bolgov, Polym. Eng. Sci. 24 (1984) 1396.
[14] E. Urbanovici, E. Segal, Thermochim. Acta 171 (1990) 87.
[15] B. Wunderlich, Macromolecular Physics, Vol. 2, Academic Press, New York, 1976, pp. 132–147.
[16] J.N. Hay, Brit. Polym. J. 3 (1971) 74.
[17] P. Supaphol, J.E. Spruiell, J. Macromol. Sci. Phys. B39 (2000) 257.
[18] P. Supaphol, SPE-ANTEC Proc. 2000, 1631.
[19] K. Ravindranath, J.P. Jog, J. Appl. Polym. Sci. 49 (1993) 1395.
[20] J.J.C. Cruz-Pinto, J.A. Martins, M. Oliveira, J. Colloid Polym. Sci. 272 (1994) 1.
[21] E. Urbanovici, H.A. Schneider, D. Brizzolara, H.J. Cantow, J. Therm. Anal. 47 (1996) 931.
[22] J.N. Hay, M. Sabir, Polymer 10 (1969) 203.
[23] J.N. Hay, P.A. Fitzgerald, M. Wiles, Polymer 17 (1976) 1015.
[24] J.N. Hay, Brit. Polym. J. 11 (1979) 137.
[25] P. Supaphol, J.E. Spruiell, Polymer 42 (2001) 699.
[26] P. Supaphol, J.E. Spruiell, J. Appl. Polym. Sci. 75 (2000) 337.
[27] E. Kreyszig, Advanced Engineering Mathematics, 7th Edition, Wiley, New York, 1993.
[28] P. Supaphol, J.E. Spruiell, Polymer 41 (2000) 1205.
[29] H. Janeschitz-Kriegl, E. Ratajski, H. Wippel, Colloid Polym. Sci. 277 (1999) 217.
[30] F.P. Price, in: A.C. Zettlemoyer (Ed.), Nucleation, Marcel Dekker, New York, 1969, Chapter 8.
[31] B. Wunderlich, Macromolecular Physics, Vol. 2, Academic Press, New York, 1976, Chapter 5.
[32] J.D. Hoffman, G.T. Davis, J.I. Lauritzen Jr., in: N.B. Hannay (Ed.), Treatise on Solid State Chemistry, Vol. 3, Plenum Press, New York, 1976, Chapter 7.
[33] J.D. Hoffman, R.L. Miller, Polymer 38 (1997) 3151.
[34] P. Supaphol, J.E. Spruiell, J. Appl. Polym. Sci. 75 (2000) 44.
[35] P. Supaphol, J.J.-J. Hwu, P.J. Phillips, J.E. Spruiell, SPE-ANTEC Proc. 1997, 1759.